

Review | Received 22 March 2024; Accepted 29 April 2024; Published 9 May 2024  
<https://doi.org/10.55092/am20240005>

# Rheology as a versatile tool in concrete technology: a mini-review

Xintong Guo<sup>1</sup>, Dengwu Jiao<sup>1,2,\*</sup>

<sup>1</sup> Department of Architecture and Civil Engineering, City University of Hong Kong, Kowloon, Hong Kong SAR, China

<sup>2</sup> City University of Hong Kong Shenzhen Research Institute, Shenzhen 518057, Guangdong, China

\* Correspondence author; E-mail: dengjiao@cityu.edu.hk (D. JIAO).

**Abstract:** The rheological characteristics of concrete offer insights into characterizing the flowability and finishability, predicting the placement and casting, as well as exerting significant influence on the mechanical properties and durability. This paper presents a brief overview on the applications of rheological properties in cement and concrete science and technology. The methods for designing and optimizing concrete mixtures based on the rheology of cement paste and/or concrete are summarized. The evaluations of structural evolutions of cementitious paste after the contact of water with cementitious particles, and the determination of setting time utilizing rheological properties, are discussed. The applications of rheological properties in transporting, pumping, placement, and casting processes are also illustrated based on the relationships between rheological parameters (*i.e.*, yield stress, plastic viscosity, and degree of thixotropy) and concrete properties such as stability, pumpability, formwork pressure and mechanical strength between multi-layers. Additionally, the correlations between rheological properties and 3D printing parameters are also briefly highlighted.

**Keywords:** Rheology; mixture design; structural build-up; stability; pumpability; formwork casting; 3D concrete printing

## 1. Introduction

Fresh cement-based materials can be regarded as complex suspensions, encompassing grain sizes ranging from microns to centimeters. The fresh properties of concrete play significant roles in practical engineering applications. Without adequate fresh properties, even the most carefully engineered structural concrete is at risk of failure due to the difficulties in filling molds and compacting the material around the reinforcing steel [1,2]. Traditional methods for assessing workability, such as slump, V-funnel, or L-box tests, often all short in fully distinguishing the various aspects of fresh properties of concrete [3]. For example, fresh concrete with different rheological parameters may yield similar results in V-funnel or L-box tests. Consequently, the fresh properties of concrete may be potentially misinterpreted. To mitigate these discrepancies, it is necessary to characterize the fresh properties of concrete using fundamental physical quantities.



Copyright©2024 by the authors. Published by ELSP. This work is licensed under Creative Commons Attribution 4.0 International License, which permits unrestricted use, distribution, and reproduction in any medium provided the original work is properly cited.

Rheology, the study of flow and deformation of matter [4], is particularly relevant in the field of cement and concrete. It mainly examines the evolution of viscosity, plasticity, and elasticity properties in cement-based materials when subjected to shear stress or strain. Yield stress and plastic viscosity are the two fundamental rheological parameters, with the former denoting the minimum shear stress required to initiate flow, and the latter characterizing the relationship between shear stress and shear rate during steady flow conditions [5,6]. The utility of rheology extends beyond merely assessing flow and deformation. It serves as an effective tool in numerous engineering applications related to concrete. These include concrete mixture design, assessing workability, and predicting the flow behavior and stability [7-9]. Additionally, other rheological parameters such as static yield stress (which correlates with the colloidal interactions and rigid links among solid particles [10-12], typically assessed through stress growth tests) and storage modulus (indicative of material elastic behavior [13,14], which is determined by small amplitude oscillatory shear tests), offer insights into the evaluations of structural build-up and setting time of cement-based materials [15-17]. All these properties have significant effects on the mechanical strength, shrinkage, pore structure, and durability of hardened concrete [18-22]. This paper presents a critical review of the applications of rheological properties in the aforementioned areas. Furthermore, the correlations between rheology and printability of 3D printing concrete are also briefly discussed.

## 2. Guiding mixture design of concrete

### 2.1. Mixture design based on paste rheology

Rheology finds significant applications in the design of concrete mixtures, particularly in the self-compacting concrete. While various mix design and optimization methods for self-compacting concrete have been proposed, such as empirical design methods, statistical factorial models, closed aggregate packing methods, and artificial neural networks, each possesses distinct advantages alongside common drawbacks, notably involving high labor, time, and material costs [23,24]. Furthermore, none of these methods fully meet the requirements for widespread applicability, robustness, technical soundness, sustainability, and economic viability [25]. Therefore, researchers have recently been increasingly exploring the rheological perspective in self-compacting concrete design.

Saak *et al.* [26] introduced the “rheology of paste model” as a framework for designing the mix proportions of self-compacting concrete. The model operates on the principle that a single spherical particle can be suspended, thereby avoiding both dynamic and static segregations. Through this, a series of theoretical relationships between rheological parameters and density difference can be established to ascertain the minimum yield stress and viscosity of cementitious paste. The upper bounds of yield stress and viscosity are experimentally calibrated based on the critical state of poor deformability of concrete. Consequently, a suitable range of rheological properties can be determined. Subsequently, the rheology of paste model was expanded by Bui *et al.* [27] by incorporating considerations of volume and particle size distribution of aggregates. Moreover, Ferrara *et al.* [28] further extended this model to encompass the preparation of steel fiber reinforced self-compacting concrete. The rheology of paste model offers the potential to significantly reduce laboratory work and materials, thus providing a theoretical foundation for quality control in concrete production.

Generally, fresh self-compacting concrete is commonly conceptualized as a two-phase material consisting of mortar and coarse aggregate, with mortar representing fine particles suspended in cement

paste [29, 30]. On this basis, An *et al.* [31-33] introduced another widely adopted mixture design method for self-compacting concrete, according to the correlations between rheological properties of paste or mortar, water-to-cement ratio and superplasticizer content at fixed aggregate levels and physical properties. By establishing a series of equations, as described in Eq. (1) and Eq. (2), the self-compacting area of paste and mortar could be easily obtained using this design procedure without reliance on mathematical software.

$$\tau_{mortar} \leq \frac{\sqrt{2}\Delta\rho \cdot gr^2}{3\delta_{mortar}} \quad (1)$$

$$\eta_{mortar} \geq \frac{2r^2 g \cdot \Delta\rho \cdot T_f}{9H} \quad (2)$$

Where  $\tau_{mortar}$  and  $\eta_{mortar}$  are the yield stress and viscosity of the mortar, respectively;  $\Delta\rho$  is the density difference between coarse aggregates and suspending mortar;  $g$  is the gravitational acceleration;  $T_f$  is the flowing time;  $H$  is the height of the slump cone;  $r$  is the average radius of coarse aggregates, and  $\delta_{mortar}$  is the excess mortar film thickness. Notably, this approach not only provides an efficient means to predict the workability of self-compacting concrete based on the paste rheology, but also significantly reduces laboratory work and time. However, considering the significant influence of aggregate content and physical properties on the rheological properties and workability of concrete, it is essential to incorporate aggregate parameters when establishing the theoretical models. Consequently, Zhang *et al.* [34] explored the effect of coarse aggregate on self-compacting concrete to establish a new theoretical framework. Building upon the previously proposed model, this study accounts for gradation characteristics and contents of gravel and sand. Furthermore, Li *et al.* [35] improved the mixture design method of self-compacting concrete containing fly ash and limestone powder ternary binder materials based on the paste threshold theory. More details are referred to [36].

## 2.2. Mixture design based on concrete rheology

Utilizing a graph depicting yield stress against plastic viscosity proves to be an effective approach for describing the complex variations of rheological parameters. Wallevik *et al.* [37] introduced the “workability box” technique for concrete mixture design. The workability box consists of several distinct regions without an exact and clear boundary, each representing an optimal range of yield stress and plastic viscosity for specific concrete applications. The workability box is tailored to different concrete types and their intended use. For example, Xie *et al.* [38] suggested that the suitable parameters for the C20 concrete fall within a yield stress range of 300 - 1500 Pa and a plastic viscosity range of 11 - 43 Pa.s. Integrating the workability box with rheography (as depicted in Figure 1) serves as crucial tool in achieving well-proportioned concrete mixtures concerning flowability, stability, robustness, and cost-effectiveness [37]. From a scientific standpoint, this approach demonstrates how to optimize mixture proportions based on site-specific concrete properties. It should be noted that the individual effects by altering concrete composition are additive [39], a concept known as the vectorized-rheograph approach. The results indicate that the proportion design method based on the concrete rheological properties was both convenient and practical.

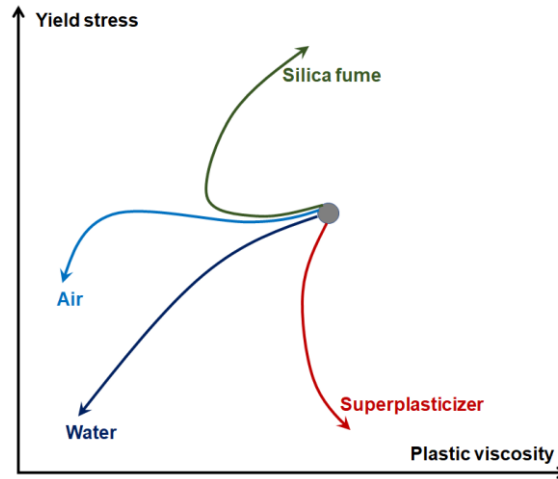


**Figure 1.** Effect of ingredients on concrete rheological properties (Copyright© 2010 Elsevier Ltd. All rights reserved).

Based on rheological properties, Jiao *et al.* [40] employed the simplex centroid design method to optimize and determine aggregate content, cementitious content, and the composition of the cementitious system. Through this method, the optimum content of total cementitious materials in concrete could be determined by considering the relationships between workability and rheological parameters at various paste volume fractions. The contours for slump value, yield stress, plastic viscosity, and compressive strength were established, and several critical lines for each property could be acquired to meet the required values, as illustrated in Figure 2. The overlapping area of these critical lines in Figure 2 was identified as the optimal combination of cementitious materials composition. The findings demonstrated that it was an effective way to optimize the mixture design of concrete based on the rheological properties using the simplex centroid design method. Moreover, this proposed methodology has been extended to design high-performance concrete with multiple performance requirements [41,42].

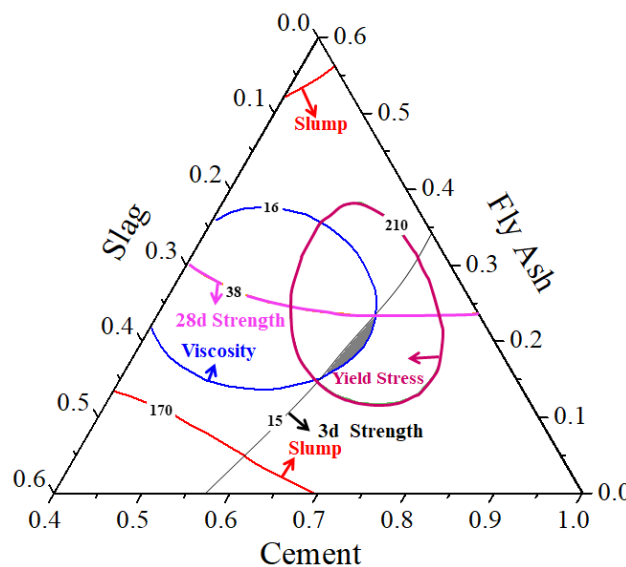


**Figure 2.** Optimization of cementitious materials composition (Copyright© 2018 published by Elsevier).

### 3. Characterizing the structural build-up and setting time

Understanding the structural development throughout the setting phase of concrete is essential in the successful placement and formwork removal. The traditional methods for determining setting time, such as Vicat test [43], hydraulic pressure variation [44], and heat of hydration observed by acoustic wave propagation [45], or electrical conductivity [46], lack direct correlation with field conditions. These measurements are somewhat arbitrary and do not directly address the fundamental phenomena such as stress and deformation. The rheological properties of fresh concrete are influenced by cement hydration and chemical interactions in the cement paste system, as well as the morphology and gradation of fine and coarse aggregates in the mixture [5]. The properties of fresh concrete undergo changes from a fluid to a solid, starting from the initial contact of water and cement. A typical evolution of yield stress over time, obtained from stress growth test, is shown in Figure 3. It can be observed that the yield stress increased slowly during the dormant period, followed by a pronounced rapid increase once the accelerating period begins [47]. This can be attributed to the enhanced contact bonding due to cement hydration and increasing frictional forces between solid particles [48,49]. Consequently, Point B, corresponding to the significant increase in yield stress, serves as a marker for identifying the initial setting time of concrete materials.

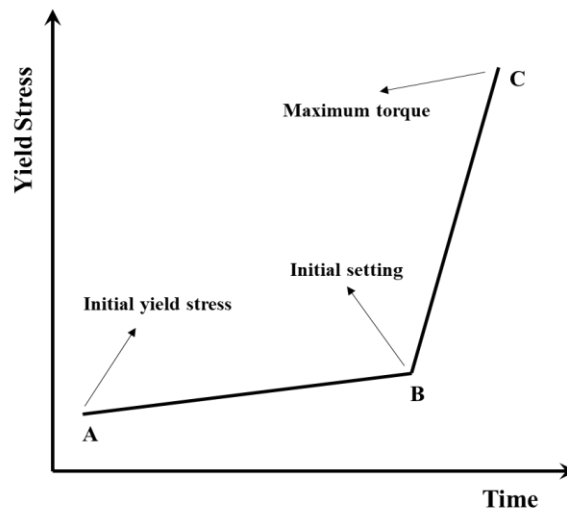


**Figure 3.** Evolution of yield stress over time (Copyright© 2008 Elsevier Ltd).

From a quantitative viewpoint, the structural build-up of cementitious materials can be estimated based on the developments of static yield stress, as depicted in Eq. (3) [51] and Eq. (4) [52] for a linear and exponential evolution of static yield stress, respectively.

$$\tau_0(t) = \tau_0 + A_{thix} \cdot t \quad (3)$$

$$\tau_0(t) = \tau_0 + A_{thix} \cdot t_c (e^{t/t_c} - 1) \quad (4)$$

Where  $\tau_0$  and  $\tau_0(t)$  are the yield stress at beginning and resting time  $t$ , respectively.  $A_{thix}$  is the structural build-up rate, and  $t_c$  is a characteristic time for achieving the best fit with experimental values.

Struble and Leit [47] pointed out that the setting time identified through rheological tests closely aligned with the end of the dormant period measured by calorimetry, and it also exhibited a reasonable

correlation with the initial setting time determined using Vicat test. Amziane and Ferraris [48] believed that the rheology and hydraulic pressure methods offer advantages of monitoring the setting evolution from the moment of mixing, unlike the widely used Vicat measurement, which shows no changes until the initial set. Similarly, Ferraris and Taylor [53] reported that the setting time measured via stress growth test was approximately 33% lower than that measured using Vicat needle. Sant *et al.* [50] observed that the initial setting time of plain cement paste with w/c of 0.3 measured through yield stress was 4.2 hours, followed by an additional 1.8 hours for the value identified by Vicat measurements. Furthermore, Bentz and Ferraris [54] noted that the rheological measurement provided the advantage of potentially earlier performance evaluation compared to conventional Vicat needle penetration tests on cement pastes. Therefore, the yield stress derived from the stress growth curve serves not only to determine the setting time but also to monitor the structural development of cement-based materials before initial setting.

## 4. Predicting placement and casting processes

### 4.1. Stability

Stabilities, including dynamic stability and static stability, are the primary required performances for fresh concrete, especially for highly flowable concrete and self-compacting concrete. The dynamic stability relates to its resistance against segregation during transportation and placement, while the static stability refers to the resistance to segregation and bleeding of fresh concrete at rest state [55]. It should be noted that there is a limited correlation between dynamic and static stability. In other words, fresh concrete with suitable static stability does not mean that the concrete possesses adequate dynamic stability [56]. The lack of stability can lead to various issues in concrete production such as bleed channels and honeycombing, which can compromise the quality of the interface, permeability, and mechanical properties of hardened concrete. Therefore, it is utmost importance to characterize, predict, and control the stability of fresh concrete during the transportation, pouring, and casting.

Fresh concrete can be conceptualized as a suspension consisting of paste and aggregate particles. The force exerted by the matrix on a moving particle includes both viscous drag arising from viscous friction and form drag resulting from boundary layer separation in the wake of particle movement [57]. Assuming that the particle is roughly spherical, the terminal velocity of a solid sphere sinking in a Newtonian fluid with a density lower than that of the solid can be calculated using Stoke's equation [58-60], as shown in Eq. (5).

$$u_t = \frac{2}{9} \cdot \frac{g(\rho_s - \rho_f)R^2}{\mu} \quad (5)$$

Where  $u_t$  is the terminal velocity of a moving sphere,  $R$  is the radius of the sphere,  $\rho_s$  and  $\rho_f$  are respectively the density of sphere and fluid,  $g$  is the acceleration gravity, and  $\mu$  is the viscosity of the Newtonian fluid. In a non-Newtonian fluid with yield stress, it is possible that the solid may not sink at all, even if its density exceeds that of the fluid. Indeed, Beris *et al.* [57] pointed out that a spherical particle would only settle in a Bingham plastic fluid when the dimensionless yield stress parameter  $Y_g$ , as defined by Eq. (6), is less than 0.143.

$$Y_g = \frac{3 \cdot \tau_0}{2R \cdot (\rho_s - \rho_f) \cdot g} \quad (6)$$

Where  $\tau_0$  is the yield stress of the fluid. From Eq. (2), it is evident that the sedimentation of solid particles initiates once the yield stress falls below a critical threshold. In other words, the point at which a particle begins moving relative to the medium, known as the threshold drag force, is solely determined by the yield stress and unaffected by fluid viscosity. Following the onset of settling, the velocity of spherical particle movement in a Bingham fluid can be derived from Eq. (5), under the assumption that the corresponding Reynolds number is very small, which was accepted by Refs. [59-61]. Nevertheless, He *et al.* [58] stated that the fluid drag forces acting on a sphere within a non-Newtonian fluid were jointly determined by both the yield stress and viscosity, with the dominance of yield stress particularly pronounced for fine particles. Consequently, the terminal velocity of solid particle settling in a Bingham plastic fluid can be derived from the following equation:

$$\frac{\eta_{pl} u_t}{2R} + \tau_0 = \frac{g(\rho_s - \rho_f)R}{9} \quad (7)$$

Where  $\eta_{pl}$  is the plastic viscosity of the Bingham fluid. When considering fresh concrete as a two-phase composite material, it becomes evident from Eqs. (5-7) that the initiation of motion of coarse aggregate within fresh concrete depends on several key parameters, including the yield stress of the mortar, the disparity in density between the coarse aggregate and the mortar matrix, and the size of the coarse aggregate. Once settlement occurs, factors such as the plastic viscosity of the Bingham fluid becomes significant contributors to the velocity of sphere particles. Based on the particle settlement theory, it is evident in the literature that the rheological parameters such as yield stress, plastic viscosity, and the degree of thixotropy exert notable influences on both dynamic stability [56,62-63] and static stability [64-67].

Recently, Hosseinpoor *et al.* [68] investigated the static and dynamic stability of self-compacting concrete, employing a biphasic approach that integrates the rheological characteristics of fine mortars and morphology of coarse aggregates. In the context of static stability, they introduced two criteria, with a pivotal focus on the behavior of particles within Stoke's flow region. The relative velocity of the settling particles with respect to the suspended slurry should approach zero in the absence of any segregation. Therefore, the concept of critical diameter  $d_c$  was introduced, as derived from the Eq. (8):

$$d_c = \frac{K \cdot \tau_0}{|\rho_s - \rho_f| g} \quad (8)$$

Where  $K$  is the shape correlation factor of particles (a value of 18 is selected for a sphere). Particles are considered stable when their size falls below the critical diameter. Conversely, when the particle diameter exceeds the critical diameter, stability is determined by calculating the critical solid fraction using Eq. (9).

$$\phi_c = \frac{\phi_{\max}}{\sqrt[3]{\frac{6M \cdot \tau_0}{\pi |\rho_s - \rho_f| \cdot d \cdot g} + 1}} \quad (9)$$

Where  $M$  is a shape-dependent parameter, which is equal to  $3\pi/4$  for identical spherical particles,  $\phi_c$  and  $\phi_m$  are the critical solid fraction and the maximum random packing fraction, respectively, and  $d$  is the diameter for a spherical particle. Results indicate that the yield stress and plastic viscosity of fine

mortar serve as the primary rheological factors governing the stability of SCC, and improving the visco-elastoplastic properties of fine mortar is found to enhance the dynamic stability of SCC. Therefore, optimizing the rheological properties of fine mortar is regarded as a key strategy for effectively improving the construction performance of self-compacting concrete. Note that the vibration or shearing process can somewhat reduce the viscosity of cement paste, resulting in shear thinning behavior [69,70]. This phenomenon also significantly influences the stability of suspended aggregates in cement paste.

#### 4.2. Pumpability

Pumping is a widely utilized method for casting concrete globally, facilitating rapid and efficient concrete placement. The pumpability of concrete refers to its ability to be mobilized and stabilized under pressure while retaining its original properties. However, when subjected to pressure, fresh concrete is prone to aggregate segregation, which usually leads to hose blockage. Another challenge associated with pumping is the alteration of the air void system [71]. Despite numerous efforts by researchers to establish relationships between concrete velocity and the friction of concrete against pipe walls, there remains a lack of approaches that incorporate a dynamic element into pumping models to account for the behavior of concrete in motion. Fortunately, the rheological behavior of fresh concrete is an efficient and useful way to characterize the pumpability ideally, given that rheology is the study of deformation and flow of matter. Additionally, the field of tribology, which focuses on the studies of the interaction of surfaces in relative motion, has also been integrated with rheology in the context of pumping.

Considering both the rheological and tribological properties, Kaplan [72] introduced a bi-linear model that correlates the required pumping pressure with the actual flow of concrete, as illustrated in Figure 4. The model describes two distinct regions. The first portion, characterized by lower concrete velocities, is solely influenced by the interface properties, while the second portion necessitates consideration of both the interface properties and the flow properties of the concrete to predict pumping pressure accurately. Therefore, at relatively lower velocities, concrete moves as a plug flow with only a thin thickness of paste lubricating the walls. As the velocity increases, the pressure imposed on the central portion of the plug becomes sufficient to initiate flow, transitioning into a viscous flow within the concrete. After examining the velocity profiles of pressure loss versus discharge rate curve, the left side is governed primarily by the properties of the lubrication layer, while the right side considers both the lubrication layer properties and the bulk concrete properties in determining pumping parameters.

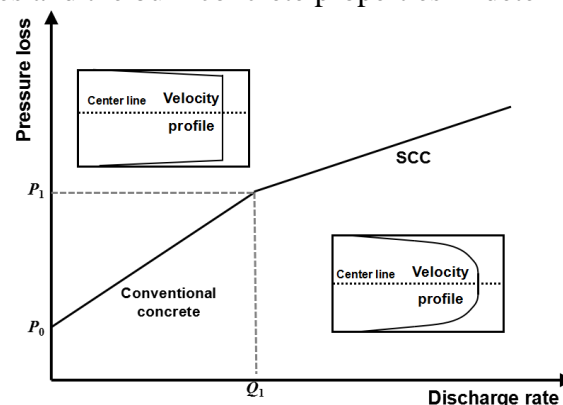


**Figure 4.** Pressure loss versus discharge rate under different conditions (Copyright© adapted from Kaplan D).

Conventional concrete typically exhibits a higher yield stress, predominantly situating it in the left zone of the bi-linear model, whereas self-compacting concrete, with its lower yield stress, typically falls into the right zone. Nevertheless, Feys *et al.* [73] found that a lubrication layer near the wall was also formed in self-compacting concrete, with a significant portion of the concrete experiencing shearing due to the lower yield stress. Considering the presence of lubricating layer, Kwon *et al.* [74] derived equations to calculate the flow rate of concrete in the pipe. The typical velocity profile within the pipe flow of pumped concrete is illustrated in Figure 5. The shear stress induced by the flow results in a shear rate both within the lubricating layer and within the concrete itself. The flow rate can be determined by calculating the velocity of the pumped concrete using Eq. (10):

$$Q = \frac{150\pi}{\mu_S \mu_P} \cdot \left[ 3\mu_P \Delta P (R_P^4 - R_L^4) - 8\tau_{S,0} \mu_P (R_P^3 - R_L^3) \right] + 3\mu_S \Delta P (R_L^4 - R_G^4) - 8\tau_{P,0} \mu_S (R_L^3 - R_G^3) \quad (10)$$

Where  $Q$  is the flow rate,  $R_L$  and  $R_G$  are the distance from the center of the pipe to the lubricating layer and the radius at which the shear rate begins, respectively,  $\tau_{S,0}$  and  $\tau_{P,0}$  are the yield stress of the lubricating layer and the bulk concrete, respectively, while  $\mu_S$  and  $\mu_P$  are the plastic viscosity of the lubricating layer and the bulk concrete, respectively. From Eq. (10), it can be observed that the flow rate is directly related to the rheological properties of both the lubricating layer and the pumped concrete, along with the radius of the pipe and the pressure loss during pumping.

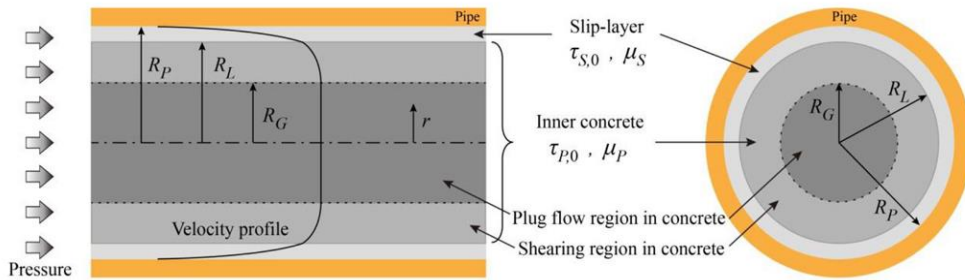


**Figure 5.** Typical velocity profile of pumped concrete inside a pipe (Copyright© 2013 ACI Materials).

It should be noted that the flow rate determined according to Eq. (10) is based on the Bingham model, ignoring the shear thickening behavior of lubrication layer and concrete. High-performance concrete and self-compacting concrete with large paste volume typically exhibit shear thickening behavior, due to the order-disorder transitions and the formation of hydro-clusters [75,76]. The shear thickening intensity depends on mixture proportions (such as granular aggregates, mineral additives, and chemical admixtures) [77-79], and external factors (e.g., temperature, pressure, and shear rate) [80-82]. In this context, Zhaidarbek *et al.* [83] recently analyzed the flow characteristics of concrete pumping after encompassing Herschel-Bulkley and modified Bingham fluids, thereby addressing the shortcomings of Eq. (10). The analytical expression of the flow-pressure drop relationship, shear rate distribution and velocity field distribution for the Herschel-Bulkley fluid is shown in Eq. (11).

$$R_{HP}(\bar{\eta}, R, G) = \pi R^2 u_{plug} \left[ 1 - \frac{2n}{3n+1} \left( 1 + \frac{n}{2n+1} \frac{\tau_0}{\tau_{wall}} \right) \left( 1 - \frac{\tau_0}{\tau_{wall}} \right) \right] \quad (11)$$

For the modified Bingham fluid, the flow rate can be described as Eq. (12).

$$\begin{aligned}
Q_{HP}(\bar{\eta}, R, G) = & \frac{\pi R^3}{840 A_2^4 \tau_{wall}^3} [-\mu_p^7 + W \mu_p^6 + 140 \mu_p A_2^3 (\tau_0^3 - \tau_{wall}^3) \\
& - 2W \mu_p^4 A_2 (\tau_{wall} + 6\tau_0) + 14 \mu_p^5 A_2 \tau_0 \\
& - 70 \tau_0^2 A_2^2 \mu_p^3 - 8W A_2^3 \tau_{wall} \tau_0 (3\tau_{wall} + 4\tau_0) \\
& + 2W \mu_p^2 A_2^2 (3\tau_{wall}^2 + 24\tau_0^2 + 8\tau_{wall} \tau_0) \\
& + 120W A_2^3 \tau_{wall}^3 - 64W A_2^3 \tau_0^3]
\end{aligned} \tag{12}$$

Where  $u_{plug}$  is the velocity of the plug flow near the center of the pipe;  $n$  is flow index in the Herschel Bulkley model;  $R$  is the pipe radius;  $\tau_0$  is the initial shear stress;  $\tau_{wall}$  is the shear stress near the wall;  $\eta_p$  is the plastic viscosity in the modified Bingham model;  $A_2$  is the second-order coefficient in the modified Bingham model, and  $W$  is a parameter related to the second-order coefficient and the shear stress. The experimental results demonstrate that the modified Bingham model is more suitable for simulating the nonlinear characteristics between shear stress and shear rate of self-compacting concrete, particularly in determining the yield stress [83]. Note that the pumpability depends on the rheological parameters, and conversely, the pumping process also exert a significant influence on the rheology of bulk concrete [84–88], which should be considered when evaluating the relationships between pumpability and rheological properties.

#### 4.3. Formwork pressure

Formwork pressure exerted by the concrete is of great interest in construction because it affects the construction cost, speed, and safety. With the increasing adoption of highly flowable concrete and self-compacting concrete, it is important to gain a comprehensive understanding of actual formwork pressure. Generally, formwork pressure is influenced by various factors such as casting procedure, ambient and concrete temperatures, aggregate sizes, admixtures, rheological properties, setting time of fresh concrete, and formwork parameters themselves [89]. Furthermore, the formwork pressure is also associated with the concrete types. For example, self-compacting concretes exerts a higher pressure on the formwork compared to conventional concrete [90]. Accurately determining the lateral pressure exerted by freshly cast concrete is essential for optimizing formwork costs and ensuring efficient construction processes. Currently, the estimation of formwork pressure for self-compacting concrete relies on the hydrostatic pressure theory [89], often resulting in significantly higher calculated pressures compared to actual values. In this context, Vanhove *et al.* [91] proposed a predictive model for the lateral pressure exerted by fresh concrete on formwork utilizing the Janssen model and assuming a constant friction coefficient, which is expressed as:

$$P'(h) = \frac{\rho g A}{\alpha (2e + 2L) \mu K} \cdot \left( 1 - \exp^{-\frac{(2e+2L)\mu K h}{A}} \right) \tag{13}$$

Where  $\rho$  is the density of concrete,  $g$  is the acceleration due to gravity,  $A$ ,  $e$ , and  $L$  are the area, thickness, and width of the formwork, respectively, and  $\alpha$  is the friction coefficient. However, the yield stress of concrete was overlooked in this equation. Additionally, it assumed no movement between the concrete and the formwork wall at the end of casting. Therefore, the calculated lateral pressure based on Eq. (13) underestimated the real pressure in the formwork, leading to an overestimation of the actual pressure in the formwork. To address these shortcomings, Eq. (13) can be modified as follows:

$$P_{concrete} = \frac{\rho g A - \alpha \tau_0 (2e + 2L)}{\alpha (2e + 2L) \mu K} \cdot \left( 1 - \exp^{-\frac{\alpha (2e + 2L) \mu K}{A} h} \right) \quad (14)$$

Where  $\tau_0$  is the yield stress of the concrete. Based on the experimental results, the modified approach based on the Janssen's model appeared promising. However, the friction coefficient should be adjusted by additional on-site tests following a strict protocol, and the thixotropic behavior of fresh concrete was not accounted for. Considering that fresh concrete behaves as an elastic material at stresses below the yield stress, Ovarlez and Roussel [92] proposed an alternative approach to predict the lateral pressure, also based on the Janssen model. They introduced the concept of relative pressure, which is defined as the ratio between the lateral pressure and the associated hydrostatic pressure during casting, as described by:

$$\Delta P = K \left( 1 - \frac{HA_{thix}}{\rho g e R} \right) \quad (15)$$

Where  $R$  is the casting rate, and  $A_{thix}$  is the flocculation rate of the concrete. This equation allows for the prediction of the maximum lateral stress reached during casting [51, 93]. Furthermore, it can be inferred that a higher flocculation rate of fresh concrete leads to a lower formwork pressure. In other words, self-compacting concrete with highly thixotropic behavior generally exhibits a reduced lateral pressure on the formwork.

#### 4.4. Multi-layer casting

During the placement of self-compacting concrete with a high rate of flocculation, characterized by a short time for rest and structure formation, the apparent yield stress of the material increases beyond a critical threshold, resulting in an already cast layer of this material failing to effectively mix with the subsequently cast layers [94]. This phenomenon leads to the development of a weak interface between different concrete layers, thereby significantly reducing the mechanical strength across the multi-layer structures. Furthermore, the presence of such weak interfaces can lead to increased porosity and permeability within the concrete, subsequently impacting the structural durability.

Roussel and Cussigh [95] identified the existence of a critical delay between layers casting, beyond which separated layers were created in the element, leading to a loss of mechanical strength. This critical delay is strongly dependent on the thixotropic behavior of fresh concrete, the thickness of the layers, and the surface roughness between the layers. Consequently, they proposed an analytical method allowing for a rough prediction of the critical delay. In scenarios where the thickness of the second layer exceeds 10 cm, the shear stress at the surface could be neglected compared to the effect of the weight of the second layer, particularly for highly viscous self-compacting concrete and at high flow rates [95]. To ensure the effective mixing between the layers, this stress must be higher than the apparent yield stress of the first layer. Following a resting period, the apparent yield stress of the first layer was determined as Eq. (3). Then the critical delay time, denoted as  $\Delta t_c$ , after which the two layers fail to mix adequately, can be expressed as:

$$\Delta t_c = \frac{\rho g h}{2\sqrt{3}A_{thix}} \quad (16)$$

From Eq. (16), it can be inferred that for traditional self-compacting concrete mixtures with a structuration rate ranging from 0.3 to 0.5 Pa/s, the critical delay typically falls within the range of 20 to

30 minutes. In other words, significant influences are unlikely to occur if casting the multi-layer concrete within this time frame. Furthermore, to mitigate the decrease in the interface bond strength of self-compacting concrete between layers over extended periods, Ye *et al.* [96] proposed several strategies, such as incorporating fly ash, increasing water-to-cement ratio, or utilizing a higher retarder dosage. These methods collectively work to reduce aggregation and flocculation between particles, thereby minimizing the time-dependent increase in the static yield stress. Consequently, these factors contribute to improving the interlayer connection ability of self-compacting concrete.

## 5. Rheology and 3D printing technique

3D printing concrete, an advanced additive manufacturing technique, is generally achieved by depositing concrete materials layer-by-layer in a controlled manner with reduced material waste and construction time [97-99]. The unique construction process requires the concrete to have suitable workability to ensure accurate extruding and stacking during the printing process. These requirements can be achieved by adjusting the rheological properties of concrete. Therefore, understanding the relationships between mixture proportions, rheological properties, and printability is essential for optimizing the material formulations and enhancing the overall performance of 3D printing process.

The printed concrete should have low dynamic yield stress but high static yield stress [100]. To meet the conflict requirements, Liu *et al.* [101] stated that the static yield strength of concrete should be higher than 4880 Pa to ensure the buildability. At the same time, the mixture should have a dynamic yield strength lower than 220 Pa for satisfying the pumpability. Zhang *et al.* [102] proposed a two-phase design combining mortar and coarse aggregate to optimize the performance of 3D printed concrete. The target rheological parameters and the maximum diameter of coarse aggregate are determined based on the nozzle size, the printing adaptability, and the selected printing parameters. Subsequently, the maximum volume fraction of the coarse aggregate is determined based on the static yield stress and plastic viscosity of the 3D-printed concrete, as described by the Coussot model in Eq. (17) and the Krieger-Dougherty model in Eq. (18), respectively.

$$\tau_c = \tau_m \left(1 - \frac{\phi}{\phi_L}\right)^{-n} \quad (17)$$

$$\eta_c = \eta_m \left(1 - \frac{\phi}{\phi_L}\right)^{-[\eta]\phi_L} \quad (18)$$

Where  $\tau_c$  and  $\tau_m$  are the static yield stress of 3D printed concrete and corresponding mortar phase, respectively.  $\eta_c$  and  $\eta_m$  are the plastic viscosity of 3D printed concrete and the corresponding mortar phase, respectively.  $\phi$  and  $\phi_L$  denote the volume fraction of coarse aggregate and the maximum packing fraction of aggregates,  $n$  is a coefficient relating to the property of coarse aggregate, and  $[\eta]$  is the intrinsic viscosity. From Eq. (18) and Eq. (19), it can also be inferred that both yield stress and plastic viscosity should be considered to evaluate the printability of 3D printing concrete containing coarse aggregate [102].

When exploring the possibilities of designing 3D printed concrete using rheological parameters, it is important to recognize the close connection between printability parameters and rheological properties during the printing process. Kruger *et al.* [103, 104] hypothesized that if the shear stress exceeds the static yield stress, plastic yielding will then occur, causing the printed structure to be collapsed. Based

on the bi-linear thixotropy model [105], they established the relationships between the static yield stress of the bottom layer (evaluated by the thixotropic structural build-up rate) and the normal stress exerted by the upper layers (which is originating from the gravity), as shown in Eq. (19) and Eq. (20).

$$N_L = - \left[ \frac{\tau_{D,i}}{\left(\frac{R_{thix} \cdot l_p}{v}\right) - \left(\frac{\rho \cdot g \cdot h_1}{2.10^3 \cdot F_{AR}}\right)} \right] \quad (19)$$

$$N_L = - \left[ \frac{\tau_{S,i} + \left(\frac{A_{thix} \cdot (\tau_{D,i} - \tau_{S,i})}{R_{thix}}\right)}{\left(\frac{A_{thix} \cdot l_p}{v}\right) - \left(\frac{\rho \cdot g \cdot h_1}{2.10^3 \cdot F_{AR}}\right)} \right] \quad (20)$$

Where  $N_L$  refers to the total number of layers,  $h_1$  is defined as the layer height,  $\rho$  is the material density,  $g$  is the gravitational constant,  $F_{AR}$  is the strength correction factor,  $\tau_{S,i}$  is the initial static yield stress,  $\tau_{D,i}$  is the initial dynamic yield stress,  $R_{thix}$  is the short-term re-flocculation rate,  $A_{thix}$  is the structuration rate, and  $l_p$  is the constant path length of each layer. This model can be used to accurately predict the 3D printing concrete building rates avoiding plastic collapse, where using Eq. (19) if Eq. (21) is valid, while else using Eq. (20).

$$\frac{d\tau}{dt} \geq \frac{\tau_{S,i} \cdot R_{thix}}{\tau_{S,i} - \tau_{D,i}} \quad (21)$$

The rheological behavior of 3D printed concrete not only determines its printability, but also directly affects the interlayer performance. Yao *et al.* [106] pointed out that the dynamic yield stress and the structural build-up rate are two key rheological parameters affecting the interlayer characteristics. Specifically, the interlayer bond strength and interlayer durability decreased with the increase of dynamic yield stress and structural building rate. Besides, a quantitative relationship between interlayer bond strength, dynamic yield stress, structural build-up rate, as well as the porosity and hydration degree, was established to evaluate the interlayer bonding performance of 3D printed concrete, as shown in Eq. (22).

$$\sigma = \left[ K \left(1 - \frac{\tau_{01}}{\tau_{max}}\right) \left(\frac{\tau_{02}}{A_{thix} \cdot t + \tau_{02}}\right) + b \right] \cdot \sigma_c + c \quad (22)$$

Where  $\sigma$  is the interlayer bonding strength at 28 days;  $\sigma_c$  is the compressive strength at 28 days;  $K$ ,  $b$  and  $c$  are constants;  $\tau_{01}$  is the dynamic yield stress;  $\tau_{max}$  is a limit value calculated according to the dynamic yield stress;  $\tau_{02}$  is the initial static yield stress measured by Perrot model, and  $t$  represents the print interval. Results showed that this model provides a reliable prediction of interlayer bonding properties of 3D printed concrete based on the rheological properties and compressive strength [106].

## 6. Conclusion

This article presents a brief overview on the rheology as a versatile tool in cement and concrete technology. Based on the discussions, the following conclusions can be reached.

(1) The vectorized-rheograph approach and centroid design method play an important role in optimizing the concrete mixture design, thereby enhancing the overall properties with multiple

requirements. The evolution of static yield stress and structural build-up rate could be used to characterize the setting behavior of fresh cement-based materials.

(2) The rheological parameters enable the precise prediction and control of concrete stability. The motion of coarse aggregate in fresh concrete suspensions is influenced by mortar yield stress, density difference, and aggregate particle size, while setting velocity of aggregate is also determined by the paste viscosity.

(3) The pumping flow rate and pressure loss could be predicted according to the rheological properties of lubricating layer and bulk concrete. Based on the evolution of yield stress over resting time, the lateral pressure exerted by fresh concrete on formwork could be predicted, and the critical delay between multi-layer casting could be calculated.

(4) Rheological parameters play an important role in optimizing the mixture design of 3D printing concrete. The thixotropic structural build-up is a key parameter for evaluating the buildability and interlayer bonding characteristics of 3D printed concrete.

In summary, rheology unquestionably serves as a powerful tool to guide concrete mixture design, characterize early-age structural evolution, and predict placing and casting processes. However, despite the considerable efforts already undertaken in this field, continuous research for refinement of the underlying theoretical mechanisms is required to unlock the full potential of rheology in optimizing concrete engineering practices to their utmost efficiency.

## Acknowledgments

Financial supports from the Shenzhen Science and Technology Program (JCYJ20230807115000001) and the New Research Initiative from City University of Hong Kong (9610661) are gratefully appreciated.

## Conflicts of interest

The authors declared that we have no conflicts of interest to this work. We declare that we do not have any commercial or associative interest that represents a conflict of interest in connection with the work submitted.

## Authors' contribution

Xintong Guo: Writing - Original Draft. Dengwu Jiao: Methodology, Resources, Writing - Original Draft, Writing - Review & Editing, Supervision.

## References

- [1] Banfill P. The rheology of fresh cement and concrete-rheology review. *British Society of Rheology* 2006, 61(130).
- [2] Roussel N. Understanding the Rheology of Concrete, *Elsevier* 2011.
- [3] Shi C, Yuan Q, Jiao D. Rheology of fresh cement-based materials fundamentals, measurements, and applications. CRC Press 2023.
- [4] Macosko CW, Larson RG. Rheology: principles, measurements, and applications. 1994.
- [5] Jiao D, Shi C, Yuan Q, An X, Liu Y, *et al.* Effect of constituents on rheological properties of fresh concrete-A review. *Cem. Concr. Compos.* 2017, 83:146-159.
- [6] Khayat KH, Meng W, Vallurupalli K, Teng L. Rheological properties of ultra-high-performance concrete — An overview. *Cem. Concr. Res.* 2019, 124.

- [7] Cu YTH, Tran MV, Ho CH, Nguyen PH. Relationship between workability and rheological parameters of self-compacting concrete used for vertical pump up to supertall buildings. *J. Build. Eng.* 2020, 32.
- [8] Li M, Li VC. Rheology, fiber dispersion, and robust properties of Engineered Cementitious Composites. *Materials and Structures* 2012, 46(3):405-420.
- [9] Wallevik OH. Rheology—a scientific approach to develop self-compacting concrete. *Proc. of the 3rd Int. Symp. on Self-Compacting Concrete, Reykjavik.* 2003, pp. 23-31.
- [10] Zhang J, Chen T, Gao X, Tian W, Jiao D, *et al.* Rheological concerns arising from the use of anti-freezing additives in cement mortar with/without SP and AEA for low-temperature construction. *Cem. Concr. Compos.* 2023, 142.
- [11] Han F, Li Y, Jiao D. Understanding the rheology and hydration behavior of cement paste with nickel slag. *J. Build. Eng.* 2023, 73:106724.
- [12] Qian Y, Kawashima S. Distinguishing dynamic and static yield stress of fresh cement mortars through thixotropy. *Cem. Concr. Compos.* 2018, 86:288-296.
- [13] Jiao D, De Schutter G. Insights into the viscoelastic properties of cement paste based on SAOS technique. *Constr. Build. Mater.* 2022, 357.
- [14] Jiao D, El Cheikh K, Shi C, Lesage K, De Schutter G. Structural build-up of cementitious paste with nano-Fe<sub>3</sub>O<sub>4</sub> under time-varying magnetic fields. *Cement Concrete Res* 2019, 124:105857.
- [15] Jiao D, De Schryver R, Shi C, De Schutter G. Thixotropic structural build-up of cement-based materials: A state-of-the-art review. *Cem. Concr. Compos.* 2021, 122:104152.
- [16] Mostafa AM, Yahia A. New approach to assess build-up of cement-based suspensions. *Cem. Concr. Res.* 2016, 85:174-182.
- [17] Wallevik JE. Rheological properties of cement paste: Thixotropic behavior and structural breakdown. *Cement Concrete Res* 2009, 39(1):14-29.
- [18] Wu Z, Khayat KH, Shi C. Changes in rheology and mechanical properties of ultra-high performance concrete with silica fume content. *Cement Concrete Res* 2019, 123.
- [19] Li Z, Zhang S, Zuo Y, Chen W, Ye G. Chemical deformation of metakaolin based geopolymer, *Cement Concrete Res* 2019, 120:108-118.
- [20] Li Z, Lu T, Liang X, Dong H, Ye G. Mechanisms of autogenous shrinkage of alkali-activated slag and fly ash pastes. *Cement Concrete Res* 2020, 135:106107.
- [21] Li Z, Lu T, Chen Y, Wu B, Ye G. Prediction of the autogenous shrinkage and microcracking of alkali-activated slag and fly ash concrete. *Cem. Concr. Compos.* 2021, 117:103913.
- [22] Iqbal Khan M, Mourad SM, Charif A. Utilization of Supplementary Cementitious Materials in HPC: From rheology to pore structure. *KSCE J. Civ. Eng.* 2016, 21(3):889-899.
- [23] Ashish DK, Verma SK. An overview on mixture design of self-compacting concrete. *Struct. Concr.* 2019, 20(1):371-395.
- [24] Siddique R. Self-compacting concrete: materials, properties and applications. *Woodhead Publishing* 2019.
- [25] Shi C, Wu Z, Lv K, Wu L. A review on mixture design methods for self-compacting concrete. *Constr. Build. Mater.* 2015, 84:387-398.
- [26] Saak AW, Jennings HM, Shah SP. New methodology for designing self-compacting concrete. *J. Mater.* 2001, 98(6):429-439.
- [27] Bui VK, Akkaya Y, Shah SP. Rheological model for self-consolidating concrete. *J. Mater.* 2002, 99(6):549-559.
- [28] Ferrara L, Park YD, Shah SP. A method for mix-design of fiber-reinforced self-compacting concrete. *Cement Concrete Res.* 2007, 37(6):957-971.
- [29] Ren Q, Tao Y, Jiao D, Jiang Z, Ye G, *et al.* Plastic viscosity of cement mortar with manufactured sand as influenced by geometric features and particle size. *Cem. Concr. Compos.* 2021, 122: 104163.
- [30] Ren Q, Tao Y, Jiao D, De Schutter G, Jiang Z. Rheological properties of concrete with manufactured sand: A multi-level prediction. *Cem. Concr. Compos.* 2022, 133:104647.

- [31] Wu Q, An X. Development of a mix design method for SCC based on the rheological characteristics of paste. *Constr. Build. Mater.* 2014, 53:642-651.
- [32] Nie D, An X. Optimization of SCC mix at paste level by using numerical method based on a paste rheological threshold theory. *Constr. Build. Mater.* 2016, 102:428-434.
- [33] Li P, Zhang T, An X, Zhang J. An enhanced mix design method of self-compacting concrete with fly ash content based on paste rheological threshold theory and material packing characteristics. *Constr. Build. Mater.* 2020, 234.
- [34] Zhang J, An X, Yu Y, Nie D. Effects of coarse aggregate content on the paste rheological thresholds of fresh self-compacting concrete. *Constr. Build. Mater.* 2019, 208:564-576.
- [35] Li P, Ran J, Nie D, Zhang W. Improvement of mix design method based on paste rheological threshold theory for self-compacting concrete using different mineral additions in ternary blends of powders. *Constr. Build. Mater.* 2021, 276.
- [36] Yuan Q, Shi C, Jiao D. Rheology of fresh cement-based materials: fundamentals, measurements, and applications. *CRC Press* 2022.
- [37] Wallevik OH, Wallevik JE. Rheology as a tool in concrete science: The use of rheographs and workability boxes. *Cement Concrete Res.* 2011, 41(12):1279-1288.
- [38] Xie H, Liu F, Fan Y, Yang H, Chen J, *et al.* Workability and proportion design of pumping concrete based on rheological parameters. *Constr. Build. Mater.* 2013, 44:267-275.
- [39] Banfill PFG. Additivity effects in the rheology of fresh concrete containing water-reducing admixtures. *Constr. Build. Mater.* 2011, 25(6):2955-2960.
- [40] Jiao D, Shi C, Yuan Q, An X, Liu Y. Mixture design of concrete using simplex centroid design method. *Cem. Concr. Compos.* 2018, 89:76-88.
- [41] Shi C, Jiao D, Zhang J, Wang D, Zhang Y, *et al.* Design of high performance concrete with multiple performance requirements for #2 Dongting Lake Bridge. *Constr. Build. Mater.* 2018, 165:825-832.
- [42] Shi C, Jiao D, Yuan Q. Mixture design of concrete based on rheology, 4th International Symposium on Design, Performance and Use of Self-Consolidating Concrete (SCC'2018-China), Changsha, China, 2018, pp. 3-15.
- [43] Sleiman H, Perrot A, Amziane S. A new look at the measurement of cementitious paste setting by Vicat test. *Cement Concrete Res* 2010, 40(5):681-686.
- [44] Amziane S. Setting time determination of cementitious materials based on measurements of the hydraulic pressure variations. *Cement Concrete Res* 2006, 36(2):295-304.
- [45] Carlson J, Nilsson M, Fernández E, Planell J. An ultrasonic pulse-echo technique for monitoring the setting of CaSO<sub>4</sub>-based bone cement. *Biomater.* 24(1) (2003) 71-77.
- [46] Yousuf F, Wei X, Zhou J. Monitoring the setting and hardening behaviour of cement paste by electrical resistivity measurement. *Constr. Build. Mater.* 2020, 252:118941.
- [47] Struble LJ, Lei WG. Rheological changes associated with setting of cement paste. *Adv. Cem. Based Mater.* 1995, 2(6):224-230.
- [48] Amziane S, Ferraris CF. Cementitious paste setting using rheological and pressure measurements. *Aci Mater J* 2007, 104(2):137-145.
- [49] Sun Y, de Lima LM, Rossi L, Jiao D, Li Z, *et al.* Interpretation of the early stiffening process in alkali-activated slag pastes. *Cement Concrete Res* 2023, 167.
- [50] Sant G, Ferraris CF, Weiss J. Rheological properties of cement pastes: A discussion of structure formation and mechanical property development. *Cement Concrete Res.* 2008, 38(11):1286-1296.
- [51] Roussel N. A thixotropy model for fresh fluid concretes: Theory, validation and applications. *Cement Concrete Res* 2006, 36(10):1797-1806.
- [52] Perrot A, Rängeard D, Pierre A. Structural built-up of cement-based materials used for 3D-printing extrusion techniques. *Mater Struct* 2015, 49(4):1213-1220.
- [53] Ferraris CF, Taylor PR. New approach to identify compatibility of materials for concrete related to early stiffening. 2006.

- [54] Bentz DP, Ferraris CF. Rheology and setting of high volume fly ash mixtures. *Cem. Concr. Compos.* 2010, 32(4):265-270.
- [55] Shen L, Struble L, Lange D. Modeling dynamic segregation of self-consolidating concrete. *ACI Mater. J.* 2009, 106(4):375.
- [56] Esmailkhanian B, Khayat K, Yahia A, Feys D. Effects of mix design parameters and rheological properties on dynamic stability of self-consolidating concrete. *Cem. Concr. Compos.* 2014, 54:21-28.
- [57] Beris A, Tsamopoulos J, Armstrong R, Brown R. Creeping motion of a sphere through a Bingham plastic. *J. Fluid Mech.* 1985, 158:219-244.
- [58] He YB, Laskowski JS, Klein B. Particle movement in non-Newtonian slurries: the effect of yield stress on dense medium separation. *Chem. Eng. Sci.* 2001, 56:2991-2998.
- [59] Petrou MF, Wan B, Gadala-Maria F, Kolli VG, Harries KA. Influence of mortar rheology on aggregate settlement. *ACI Mater. J.* 2000.
- [60] Petrou MF, Harries KA, Gadala-Maria F, Kolli VG. A unique experimental method for monitoring aggregate settlement in concrete. *Cement Concrete Res* 2000, 30(5):809-816.
- [61] Navarrete I, Lopez M. Estimating the segregation of concrete based on mixture design and vibratory energy. *Constr. Build. Mater.* 2016, 122:384-390.
- [62] Esmailkhanian B, Feys D, Khayat KH, Yahia A. New test method to evaluate dynamic stability of self-consolidating concrete. *ACI Mater. J.* 2014, 111(3):299-308.
- [63] Libre NA, Khoshnazar R, Shekarchi M. Relationship between fluidity and stability of self-consolidating mortar incorporating chemical and mineral admixtures. *Constr. Build. Mater.* 2010, 24(7):1262-1271.
- [64] Shen L, Struble L, Lange D. New method for measuring static segregation of self-consolidating concrete. *JOTE* 2007, 35(3):303-309.
- [65] Assaad J, Khayat KH, Daczko J. Evaluation of static stability of self-consolidating concrete. *J. Mater.* 2004, 101(3):207-215.
- [66] Wang X, Wang K, Han J, Taylor P. Image analysis applications on assessing static stability and flowability of self-consolidating concrete. *Cem. Concr. Compos.* 2015, 62:156-167.
- [67] Khayat KH, Assaad J. Relationship between washout resistance and rheological properties of high-performance underwater concrete. *J. Mater.* 2003, 100(3):185-193.
- [68] Hosseinpour M, Koura BIO, Yahia A. Rheo-morphological investigation of static and dynamic stability of self-consolidating concrete: A biphasic approach. *Cem. Concr. Compos.* 2021, 121:104072.
- [69] Zhang J, Gao X, Su Y. Influence of poker vibration on aggregate settlement in fresh concrete with variable rheological properties. *J Mater Civil Eng* 2019, 31(7):04019128.
- [70] Sanjayan JG, Jayathilakage R, Rajeev P. Vibration induced active rheology control for 3D concrete printing. *Cement Concrete Res* 2021, 140:106293.
- [71] Jolin M, Burns D, Bissonnette B, Gagnon F, Bolduc LS. Understanding the pumpability of concrete. 2009.
- [72] Kaplan D. Pumping of concretes, Ph-D dissertation (in French), Laboratoire Central des Ponts et Chaussées, Paris, 2001.
- [73] Feys D, De Schutter G, Verhoeven R, Khayat KH. Similarities and differences of pumping conventional and self-compacting concrete. *Design, Production and Placement of Self-Consolidating Concrete*, Springer 2010, pp. 153-162.
- [74] Kwon SH, Park CK, Jeong JH, Jo SD, Lee SH. Prediction of concrete pumping: part II—analytical prediction and experimental verification for prediction of pumping considering lubricating layer. *Aci Mater J* 2013, 110(6):657-667.
- [75] Jiao D, Shi C, Yuan Q. Time-dependent rheological behavior of cementitious paste under continuous shear mixing. *Constr. Build. Mater.* 2019, 226:591-600.
- [76] Feys D, Verhoeven R, De Schutter G. Why is fresh self-compacting concrete shear thickening? *Cement Concrete Res* 2009, 39(6):510-523.

- [77] Shen W, Cui H, Jiao D. Experimental observations on factors influencing shear-thickening characteristics of cement-based materials. *J. Build. Eng.* 2024, 86.
- [78] Feys D, Verhoeven R, De Schutter G. Fresh self compacting concrete, a shear thickening material. *Cement Concrete Res* 2008, 38(7):920-929.
- [79] Yahia A. Effect of solid concentration and shear rate on shear-thickening response of high-performance cement suspensions. *Constr. Build. Mater.* 2014, 53:517-521.
- [80] Jiao D, Shi C, Yuan Q, Zhu D, De Schutter G. Effects of rotational shearing on rheological behavior of fresh mortar with short glass fiber. *Constr. Build. Mater.* 2019, 203:314-321.
- [81] Jiao D, Shi C, Yuan Q. Influences of shear-mixing rate and fly ash on rheological behavior of cement pastes under continuous mixing. *Constr. Build. Mater.* 2018, 188:170-177.
- [82] Jiao D, Lesage K, Yardimci MY, Shi C, De Schutter G. Flow behavior of cementitious-like suspension with nano-Fe<sub>3</sub>O<sub>4</sub> particles under external magnetic field. *Mater Struct* 2021, 54:209.
- [83] Zhaidarbek B, Tleubek A, Berdibek G, Wang Y. Analytical predictions of concrete pumping: Extending the Khatib–Khayat model to Herschel–Bulkley and modified Bingham fluids. *Cement Concrete Res* 2023, 163:107035.
- [84] Shen W, Shi C, Khayat K, Yuan Q, Ji Y, *et al*, Change in fresh properties of high-strength concrete due to pumping. *Constr. Build. Mater.* 2021, 300:124069.
- [85] Shen W, Yuan Q, Shi C, Ji Y, Zeng R, *et al*. Influence of pumping on the resistivity evolution of high-strength concrete and its relation to the rheology. *Constr. Build. Mater.* 2021, 302.
- [86] Shen W, Yuan Q, Shi C, Ji Y, Zeng R, *et al*. How do discharge rate and pipeline length influence the rheological properties of self-consolidating concrete after pumping? *Cem. Concr. Compos.* 2021, 124:104231.
- [87] Zheng Y, Lv X, Hu S, Zhuo J, Wan C, *et al*. Mechanical properties and durability of steel fiber reinforced concrete: A review. *J. Build. Eng.* 2024, 82:108025.
- [88] Li F, Shen W, Yuan Q, Hu X, Li Z, *et al*. An overview on the effect of pumping on concrete properties. *Cem. Concr. Compos.* 2022, 129.
- [89] Gregori A, Ferron RP, Sun Z, Shah SP. Experimental simulation of self-consolidating concrete formwork pressure. *ACI Mater. J.* 2008, 105(1):97.
- [90] Wang X, Wang K, Taylor P, Morcou G. Assessing particle packing based self-consolidating concrete mix design method. *Constr. Build. Mater.* 2014, 70:439-452.
- [91] Vanhove Y, Djelal C, Magnin A. Prediction of the lateral pressure exerted by self-compacting concrete on formwork. *Mag. Concr. Res.* 2004, 56(1):55-62.
- [92] Ovarlez G, Roussel N. A physical model for the prediction of lateral stress exerted by self-compacting concrete on formwork. *Mater Struct* 2006, 39(2):269-279.
- [93] Roussel N. Rheology of fresh concrete: from measurements to predictions of casting processes. *Mater Struct* 2007, 40(10):1001-1012.
- [94] Rahman MK, Baluch MH, Malik MA. Thixotropic behavior of self compacting concrete with different mineral admixtures. *Constr. Build. Mater.* 2014, 50:710-717.
- [95] Roussel N, Cussigh F. Distinct-layer casting of SCC: The mechanical consequences of thixotropy. *Cement Concrete Res.* 2008, 38(5):624-632.
- [96] Ye H, Gao X, Zhang L. Influence of time-dependent rheological properties on distinct-layer casting of self-compacting concrete. *Constr. Build. Mater.* 2019, 199:214-224.
- [97] Buswell RA, Leal de Silva WR, Jones SZ, Dirrenberger J. 3D printing using concrete extrusion: A roadmap for research. *Cement Concrete Res.* 2018, 112:37-49.
- [98] De Schutter G, Lesage K, Mechtcherine V, Nerella VN, Habert G, *et al*. Vision of 3D printing with concrete - Technical economic and environmental potentials. *Cement Concrete Res.* 2018, 112:25-36.
- [99] Gosselin C, Duballet R, Roux P, Gaudillière N, Dirrenberger J, *et al*. Large-scale 3D printing of ultra-high performance concrete – a new processing route for architects and builders. *Mater. Des.* 2016, 100:102-109.
- [100] Yuan Q, Li Z, Zhou D, Huang T, Huang H, *et al*. A feasible method for measuring the buildability of fresh 3D printing mortar. *Constr. Build. Mater.* 2019, 227:116600.

- 
- [101] Liu Z, Li M, Weng Y, Wong TN, Tan MJ. Mixture Design Approach to optimize the rheological properties of the material used in 3D cementitious material printing. *Constr. Build. Mater.* 2019, 198:245-255.
- [102] Zhang C, Jia Z, Wang X, Jia L, Deng Z, *et al.* A two-phase design strategy based on the composite of mortar and coarse aggregate for 3D printable concrete with coarse aggregate. *J. Build. Eng.* 2022, 54:104672.
- [103] Kruger J, Zeranka S, van Zijl G. 3D concrete printing: A lower bound analytical model for buildability performance quantification. *Autom. Constr.* 2019, 106:102904.
- [104] Kruger J, Zeranka S, van Zijl G. A rheology-based quasi-static shape retention model for digitally fabricated concrete. *Constr. Build. Mater.* 2020, 254.
- [105] Kruger J, Zeranka S, van Zijl G. An ab initio approach for thixotropy characterisation of (nanoparticle-infused) 3D printable concrete. *Constr. Build. Mater.* 2019, 224:372-386.
- [106] Yao H, Xie Z, Li Z, Huang C, Yuan Q, *et al.* The relationship between the rheological behavior and interlayer bonding properties of 3D printing cementitious materials with the addition of attapulgite. *Constr. Build. Mater.* 2022, 316:125809.